EGYPTIAN DENTAL JOURNAL
www.eda-egypt.org
VOL. 71, 3051:3060, OCTOBER, 2025
PRINT ISSN 0070-9484 • ONLINE ISSN 2090-2360
ORAL MEDICINE, X-RAY, ORAL BIOLOGY AND ORAL PATHOLOGY
Submit Date : 04-07-2025 • Accept Date : 25-07-2025 • Available online: 01-10-2025 • DOI : 10.21608/edj.2025.400675.3540

EFFECT OF INTRAPERITONEAL INJECTION OF CURCUMIN NANOPARTICLES ON PAROTID SALIVARY GLANDS OF DIABETIC ALBINO RATS

Mohamed Mohamed Arafa* *and* Waleed Mohamed Shaker**

ABSTRACT

Diabetes mellitus (DM) is a prevalent disorder associated with deleterious oral manifestations, including decreased salivary flow resulting from atrophic changes in the salivary glands. Curcumin exhibits potent antioxidant, anti-inflammatory, antimicrobial and anticancer properties. However, its clinical utility is limited due to poor solubility and a short plasma half-life. Nanocurcumin (NC) overcomes these limitations by sustained release of nanoparticles. This study aimed to evaluate the effects of systemically administrated NC on the parotid glands of alloxan-induced diabetic albino rats. Twenty-four adult rats were randomly allocated into four equal groups: Control (saline injections), Diabetic-untreated (alloxan-induced diabetes, saline injections), Curcumin-treated (diabetes + curcumin), and NC-treated (diabetes + nanocurcumin). Treatments were given intraperitoneally twice daily for three weeks. At the end of the experimental period, parotid gland tissues from all groups were excised and subjected to histopathological examination using hematoxylin and eosin staining. Additionally, proliferating cell nuclear antigen (PCNA) immunohistochemistry was performed to assess cellular proliferation. Histopathological examination revealed severe atrophic changes in the parotid gland of the diabetic-untreated group. Curcumin-treated group partially restored tissue architecture, improving acinar and ductal organization while reducing vacuolation. NC-treated group showed near-normal histological features, with well-preserved acini, minimal vacuolation, and consistent basal striations. Immunohistochemical analysis of PCNA expression demonstrated significantly enhanced cell proliferation in both curcumin ($p=0.020$) and NC ($p<0.001$) treated groups compared to the diabetic-untreated group, with NC exhibiting the highest mean PCNA expression (1.83 ± 0.72). Nanocurcumin is more effective than curcumin in mitigating diabetes-induced parotid gland damage and promoting tissue regeneration.

KEYWORDS: Diabetes; Nanocurcumin; Parotid glands; PCNA; Proliferation.

* Oral Pathology Department, Faculty of Dentistry, Sinai University (Arish branch), North Sinai, Egypt.
** Oral Biology Department, Faculty of Oral and Dental Medicine, South Valley University, Qena, Egypt.

INTRODUCTION

Diabetes mellitus (DM) is a chronic metabolic disorder characterized by insulin dysfunction and deficiency, with hyperglycemia as a hallmark feature[1]. According to the International Diabetes Federation, approximately 536.6 million adults worldwide were living with DM in 2021 across 215 countries. This number is projected to rise to 783.2 million by 2045 [2]. Persistent hyperglycemia affects various tissues, including vascular, neural, renal, and glandular tissues, with significant implications for salivary glands, a crucial component of the oral cavity. Diabetic patients often experience a range of oral health issues, including an increased risk of dental caries, gingivitis, periodontitis, delayed wound healing, post-operative infections, and taste disorders[3]. These complications are strongly associated with xerostomia (dry mouth), which serves as a primary indicator of salivary gland damage caused by DM [3].

Proliferating cell nuclear antigen (PCNA) is an essential co-factor of DNA polymerase delta, critical for DNA replication and repair**.** It plays a key role in the resynthesis phase of nucleotide excision repair (NER) and base excision repair (BER) pathways [4]. In diabetic salivary gland tissues, increased PCNA expression indicates an enhanced cellular effort to repair DNA damage caused by oxidative stress, a consequence of hyperglycemia-induced metabolic disturbances [5].

Curcumin, a natural compound extracted from the turmeric plant, has gained significant attention for its therapeutic potential in managing diabetic complications due to its strong anti-inflammatory and antioxidant properties[6]. Recent studies have focused on curcumin nanoparticles, known as nanocurcumin (NC), to overcome curcumin's low bioavailability and improve its therapeutic efficacy. NC provides enhanced permeability, prolonged circulation time, resistance to metabolic degradation, and reduced toxicity associated with higher concentrations [7,8].

The effect of NC on salivary glands tissue of diabetic rats is a current hot issue in several research, but all studies tried only the oral administration of curcumin solution and NC to examine this effect [9]. Previous studies investigating the effects of NC on salivary gland tissues in diabetic models have predominantly focused on oral administration of curcumin or NC solutions. This study introduces a novel approach by utilizing intraperitoneal injections of curcumin and NC to assess their impact on the parotid glands of diabetic albino rats. The effects are evaluated through comprehensive histological and immunohistochemical analysis.

MATERIALS AND METHODS

Animal Model

A total of twenty-four healthy adult male albino rats (age: ~10 weeks, weight: 180–200 g) were included in the study. The rats were housed under controlled laboratory conditions, including a temperature of 22–25°C, adequate ventilation, a 12-hour light-dark cycle, regulated humidity and noise levels, and free access to a standard diet and water. After one week of acclimatization, the rats were randomly divided into four groups:

Group I (control group, n = 6): Healthy rats received intraperitoneal injections of saline twice daily for three weeks.

Group II (Diabetic-untreated group, n = 6): DM was induced by a single intraperitoneal injection of alloxan (140 mg/kg) [10]. After 3 days, DM was confirmed, and the rats received a single intraperitoneal injection of saline to simulate injection stress.

Similar to group II, DM was induced and confirmed in group III and IV. Then **Group III (Curcumin-treated group, n = 6)** and **Group IV (NC-treated group, n = 6)** received intraperitoneal administration of curcumin and NC, respectively, with a dose of 20 mg/kg twice daily for three weeks [11].

Induction of Diabetes mellitus (DM)

DM was induced in rats after a 12-hour fasting period by a single intraperitoneal injection of alloxan (140 mg/kg) dissolved in a 4% saline solution [10]. All alloxan-injected rats were tested for hyperglycemia after 72 hours using a glucometer with blood samples obtained from the tail vein, and only those with blood glucose levels ≥300 mg/dl were considered diabetic and included in the study. All injected rats developed diabetes and met the inclusion criteria.

Characterization of Nanocurcumin (NC)

Curcumin and NC was purchased from Nano-Gate company, Egypt. NC was characterized at the Central Laboratory Unit, Faculty of Science, South Valley University, Qena, Egypt, to confirm its nanoscale properties. NC was characterized by their particles size and surface morphology using X-ray powder diffraction (XRD), transmission electron microscope (TEM) and UV/Visible spectrophotometry. XRD patterns were recorded using a D 5000 Siemens diffractometer (Germany) with CuKα radiation (λ= 0.154178 nm). The size and shape of the obtained materials were studied using TEM (Joel Jem-1010, Japan). A computerized Analytik Jena SPECORD 200 Plus spectrophotometer (Germany) was used for studying the optical properties in the wavelength range 300-800 nm at room temperature (RT).

Tissue Preparation

At the end of the experimental period, rats were euthanized using an overdose of ketamine hydrochloride. The parotid glands were dissected, washed with saline, and fixed in 10% buffered formalin for 48 hours. Tissues were dehydrated in an ascending alcohol series, cleared in xylene, and embedded in paraffin wax. Serial sections (4–5 μm thick) were cut and stained with Hematoxylin and Eosin (H&E) for histopathological examination.

Immunohistochemical Examination

Tissue sections (4-5 μm) were mounted on positive charged slides. Using the labeled streptavidin-biotin complex method [12], mounted sections were deparaffinized in xylol for 10 min and dehydrated in a graded series of alcohol. Sections were microwaved for 10 min in 0.01 citrate buffer to unmask the antigenic sites, then treated with 0.3% hydrogen peroxide in phosphate-buffered solution (PBS) (100 μl) for 10 min at RT for endogenous peroxidase blocking. This was followed by incubation with the monoclonal anti-PCNA antibody (Dako, 1:100) for 60 min at RT, then by biotinylated secondary antibody in PBS at RT for 30 min and subsequently with streptavidin–peroxidase conjugate. Diaminobenzidine hydrochloride (DAB) was used as chromogen. Finally, the sections were counterstained by using Mayer's hematoxylin before coverslips application.

Immunohistochemical Assessment

Immunostained sections were analyzed using the IHC Profiler plugin for ImageJ, which provides automated scoring based on color deconvolution to separate DAB (brown) staining from hematoxylin (blue) counterstain. From each section, five representative fields at 40X magnification were captured. The plugin assigns staining scores based on pixel intensity: high positive (+3), positive (+2), low positive (+1), and negative (0) [13]. The average score from the five fields was calculated to represent the PCNA expression for each section.

Statistical Analysis

The data were processed and analyzed using IBM SPSS software, version 20.0. (Armonk, NY: IBM Corp). Ordinal data were summarized using descriptive statistics including minimum and maximum, mean, standard deviation, median, and interquartile range. The Kruskal Wallis test was used to compare different groups for the ordinal variable and followed by Post Hoc test (Dunn's for multiple comparisons test) for pairwise comparison. Significance of the results obtained was judged at the 5% level.

RESULTS

Nanocurcumin Characterization:

XRD was utilized to determine the crystalline nature and degree of purity of curcumin nanoparticles (Figure 1). At a diffraction angle of 2 θ, the following peaks were detected to be characteristic of the sample that had been prepared: 12.16°, 17.24°, 18.16°, 19.46°, 21.22°, 23.58°, 24.58°, 25.58°, 27.38°, 29.04°, 34.36°, 44.0°, and 77.76°. This demonstrated that the sample that was generated included crystalline curcumin [14], and the prevalence of broad peaks demonstrated that the curcumin that was obtained was of nano size. On top of that, the XRD pattern has not shown any other impurities, which is another evidence that our sample is completely free of any impurities. In order to get the average crystal size (d), Scherer's formula was utilized, and the width of the peak was used as the basis for the calculation [15]

$$d=0.9\lambda/\beta\ cos\theta$$

Given that λ represents the wavelength of the X-ray that is being utilized, β represents the full width at half maximum, and θ represents Bragg's angle of reflection. A crystallite size of 23 nanometers was used as the average for the calculation of the peaks in the XRD pattern of curcumin nanoparticles. TEM images confirm the production of spherical curcumin nanoparticles of around 17 nm in radius. The UV/Vis optical absorption spectra of the synthesized curcumin nanoparticles show a visible broadband centered at 310 nm, which is attributable to the production of curcumin in its nanoform. It is widely recognized that bulk curcumin exhibits a noticeable absorption band at 450 nm, indicating that NC typically displays a blue shift [16].

Histopathological Evaluation

Group I (control group)

Examination of the control group revealed a normal architecture of the parotid parenchyma consisting of uniform, tightly packed serous acini and collecting ducts. The acini were composed of pyramidal-shaped serous cells with spherical, basally located nuclei and basophilic cytoplasm. The intercalated ducts showed narrow lumens lined with cuboidal cells, while the striated ducts, lined with eosinophilic columnar cells, displayed central nuclei and prominent basal striations (Figure 2).

Group II (Diabetic-untreated)

Histological assessment of diabetic-untreated group showed significant atrophic changes, including prominent interacinar and interlobular spaces and thickened connective tissue septa. The acini appeared disorganized and atrophied, with indistinct cellular and acinar borders and poorly defined lumens. The acinar cells exhibited foamy and vacuolated cytoplasm, with some showing

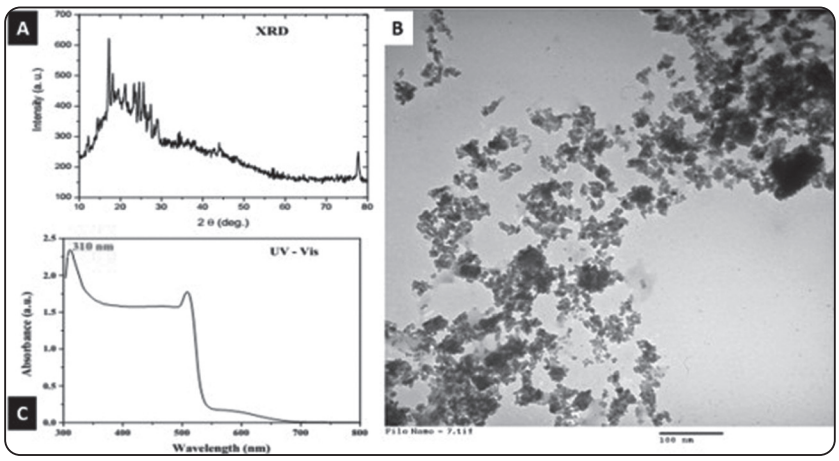

Fig. (1) Nanocurcumin characterization, (A) XDR pattern (B) TEM (C) UV/Visible spectrophotometry.

nuclear pleomorphism and hyperchromatism, while others had thin, flattened, and displaced nuclei. Fat cells were observed replacing some of the acini. The ductal structures showed enlarged, dilated lumens with disorganized epithelial lining and sign of degeneration. Striated ducts lacked basal striation and revealed cytoplasmic vacuolation (Figure 2).

Group III (Curcumin-treated)

Compared to group II, several acini and striated ducts in the curcumin treated group showed improved histological features. However, some areas still showed signs of atrophy, with pyknotic or degenerated nuclei. Certain ductal cells appeared distorted, exhibiting flattened nuclei and partially restored basal striations. Additionally, some regions retained evidence of cytoplasmic vacuolation (Figure 2).

Group IV (NC-treated)

This group displayed a histological picture closely resembled that of the control group, as the majority of the acini and ducts were well-preserved, with the epithelial lining exhibiting a uniform cellular arrangement. Instances of flattened or degenerated nuclei were minimal, and vacuolation was almost absent. In addition, Basal striations were consistently observed throughout (Figure 2).

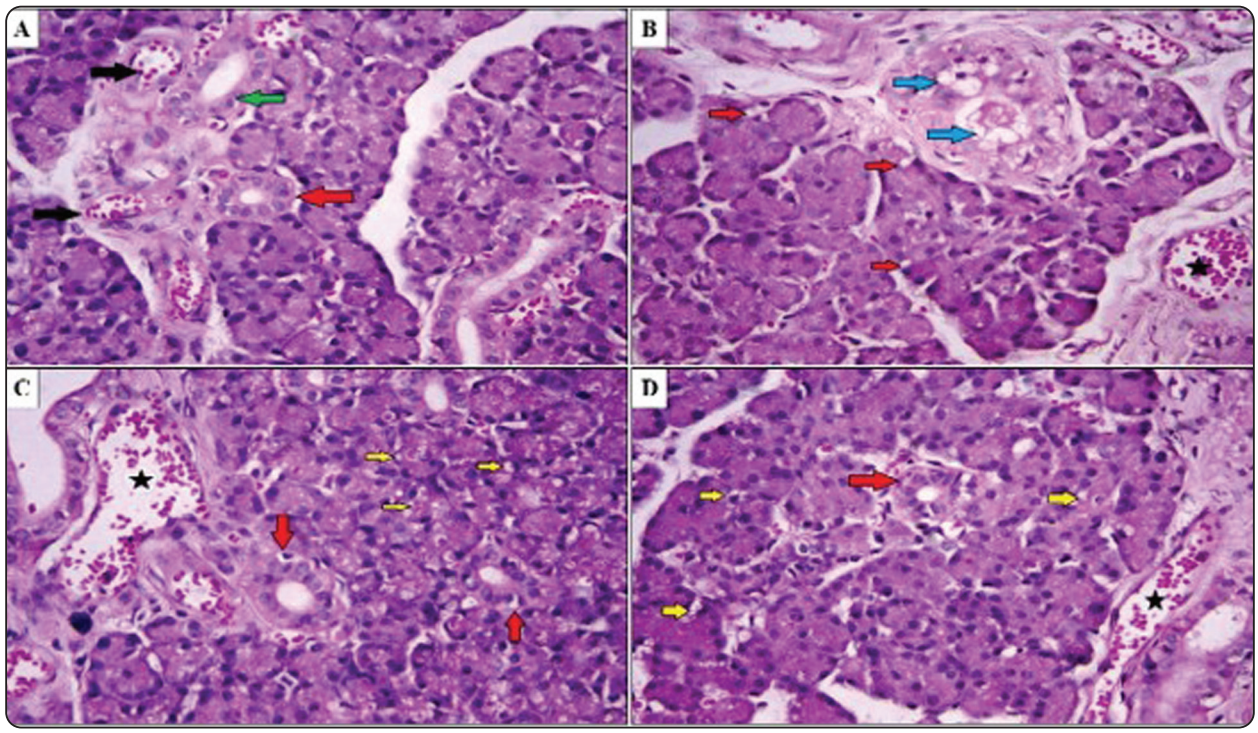

Fig. (2) Photomicrograph of parotid gland from different studied groups (H&E, X40): (A) Group I: Normal histological architecture showing well-defined serous acini with basophilic cytoplasm and basally located round nuclei. Striated ducts exhibit prominent basal striations (red arrow), interlobular ducts appear normal (green arrow), and blood vessels are normal (black arrow). (B) Group II: Severe degeneration with atrophied acini, indistinct boundaries, pleomorphic and pyknotic nuclei, intracellular vacuolation (red arrow), fatty degeneration of connective tissue septa (blue arrow), and dilated engorged blood vessels (black star). (C) Group III: Partial restoration of acinar and ductal structures, including basal striations in ducts (red arrow), reduced intracellular vacuolation (yellow arrow), and persistent dilated blood vessels (black star). (D) Group IV: Near-normal histology with uniform acinar and ductal outlines, minimal vacuolation (yellow arrow), prominent basal striations (red arrow), and less dilated blood vessels (black star).

Immunohistochemical Evaluation

The immunohistochemical analysis of PCNA expression showed distinct patterns across experimental groups. In the control group, acinar and ductal cells exhibited negative PCNA expression, with 83.3% of specimens showing negative immunostaining and 16.7% displaying low-positive (+1) staining (Figure 3), resulting in a mean value of 0.17±0.39 (Table 1). The diabetic-untreated group demonstrated predominantly negative PCNA expression in serous and ductal cells, with dispersed cells showing nuclear expression (Figure 3). Immunostaining was negative in 66.7% of specimens and low-positive (+1) in 33.3% with a mean value of 0.33 ± 0.49 (Table 1).

In the curcumin-treated group (Figure 3), nuclear PCNA expression was evident in acinar and ductal cells, with negative immunostaining in 16.7% of specimens, low-positive (+1) in 58.3%, and positive (+2) in 25%, yielding a mean value of 1.08 ± 0.67 (Table 1). The NC-treated group showed prominent nuclear PCNA expression in all specimens, with immunostaining categorized as high-positive (+3) in 16.7%, positive (+2) in 50%, and low-positive (+1) in 33.3% (Figure 3), resulting in the highest mean value of 1.83 ± 0.72 (Table 1).

The current study revealed that PCNA expression was significantly enhanced by curcumin ($p=0.020$) and NC treatments ($p<0.001$), with NC showing the greatest effect ($p=0.079$) (Table 1).

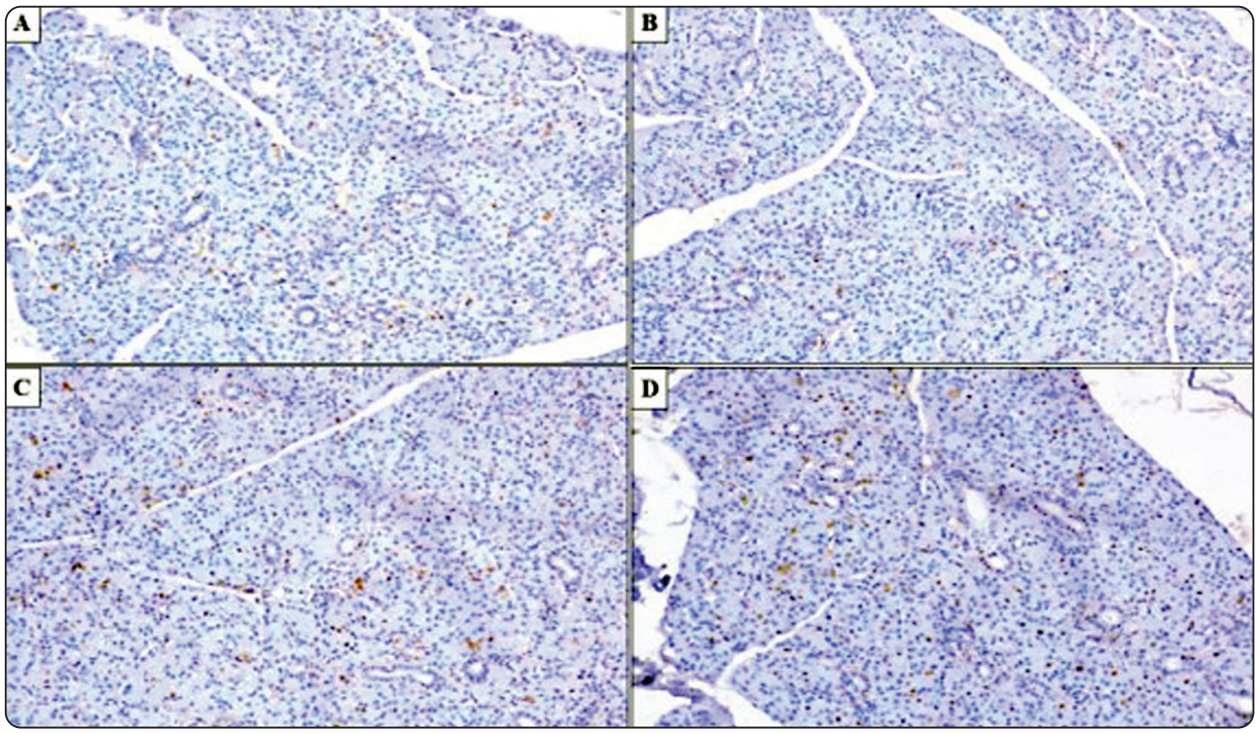

Fig. (3) Photomicrograph of immunohistochemical expression of PCNA in parotid gland from different studied groups (X20). (A) Group I: Low-positive PCNA expression, reflecting baseline proliferative activity. (B) Group II: Disparate and irregular PCNA expression, indicating variable and abnormal proliferative activity. (C) Group III: Positive nuclear PCNA expression, demonstrating increased proliferative activity compared to the control. (D) Group IV: High-positive PCNA expression, indicating robust and significantly enhanced proliferative activity.

TABLE (1) PCNA expression of the different studied groups.

	Control (n = 12)	Diabetic untreated (n = 12)	Curcumin treated (n = 12)	Nanocurcumin treated (n = 12)	H	p
PCNA						
Min. – Max.	0 – 1	0 – 1	0 – 2	1 – 3		
Mean ± SD.	0.17 ± 0.39	0.33 ± 0.49	1.08 ± 0.67	1.83 ± 0.72	27.972*	<0.001*
Median (IQR)	0 (0 – 0)	0 (0 – 1)	1 (1 – 1.5)	2 (1 – 2)		
p_0		0.565	0.004*	<0.001*		
Significance between groups	p_1=0.020*, p_2<0.001*, p_3=0.079					

***SD:* Standard deviation**

***H: H for* Kruskal Wallis test, *Pairwise comparison between each 2 groups was done using* Post Hoc Test (Dunn's for multiple comparisons test)**

p: p value for comparing between the studied groups

p_0: p value for comparing between* Control *and each other group

***p_1: p value for comparing between* Diabetic untreated *and* Curcumin treated**

***p_2: p value for comparing between* Diabetic untreated *and* Nanocurcumin treated**

***p_3: p value for comparing between* Curcumin treated *and* Nanocurcumin treated**

****: Statistically significant at p ≤ 0.05***

DISCUSSION

DM can adversely affect human salivary gland function, with the parotid gland often exhibiting greater sensitivity and more significant structural changes compared to other major glands [17]. Studies on diabetic animal models have reported that salivary hypofunction is associated with atrophy of both the parotid and submandibular glands. However, the parotid gland tends to exhibit more pronounced histopathological changes, including acinar cell atrophy, vacuolization, and ductal degeneration, indicating a higher susceptibility to diabetic complications [18].

The diabetic-untreated group in this study exhibited significant structural changes in the parotid gland, including acinar atrophy, indistinct borders, poorly defined lumens, cytoplasmic vacuolation, and nuclear abnormalities such as pleomorphism and hyperchromatism in acinar cells. These findings are consistent with those reported in several previous studies[9,19,20]. The cytoplasmic vacuolation observed in acinar and ductal cells may be attributed to the accumulation of degenerative substances and fatty degeneration within the cytoplasm [21]. Studies have reported that lipid droplets accumulate in the epithelial cells of the parotid glands due to increased free fatty acid production[22–24]. The pressure exerted by these degenerative products, primarily of a fatty nature, caused the cell boundaries to appear compressed and distorted, leading to the observed structural abnormalities [25]. Moreover, acinar cells exhibited nuclear pleomorphism and hyperchromatism. Additionally, striated ducts lacked basal striation. These changes are indicative of pre-necrotic alterations due to persistent hyperglycemia [20].

The results of the present study emphasize the effectiveness of NC in enhancing tissue architecture and cellular configuration in diabetic albino rats, compared to regular curcumin. This finding is consistent with previous studies that have reported the enhanced impact of NC on various tissues subjected to different destructive stimuli [7,26,27].

This supports the notion that NC has significant advantages over native curcumin in managing hyperglycemia, reducing oxidative stress, and improving metabolic parameters. These benefits can be attributed to NC's superior bioavailability, solubility, and cellular uptake compared to regular curcumin, which suffers from poor absorption and rapid metabolism [28]. Furthermore, it is worth noting that the intraperitoneal administration of curcumin and its nanoformulation results in much higher bioavailability compared to the oral route [29].

The immunohistochemical results of our study demonstrated negative to low-positive PCNA expression in the control group. Similarly, Elsakhawy et al. identified weak PCNA immunoreactivity in the normal parotid gland of rats, and Sumitomo et al. reported that PCNA-positive nuclei were rarely detected in normal glandular parenchyma [4,30]. This could be explained by the presence of well-differentiated cells with low proliferation index in the salivary glands [31].

Interestingly, our study revealed a significant difference in PCNA expression between the NC-treated group and the untreated group. This could be attributed to the dual role of PCNA in promoting cell proliferation and facilitating DNA repair, as part of the cellular response to mitigate damage caused by oxidative stress [32].

In the same context, we observed upregulated PCNA expression in NC-treated group as compared to curcumin-treated group, which signifies the enhanced ability of NC to promote cellular responses such as proliferation and DNA repair. This suggests that NC may offer superior protection against oxidative stress-induced damage compared to native curcumin.

In conclusion, nanocurcumin effectively rescued the diabetes-induced histopathological changes in the parotid gland, demonstrating its profound ability to promote cellular proliferation and tissue repair. This highlights its potential therapeutic role in counteracting diabetic damage in salivary glands.

Ethical Committee Approval

This study was designed in accordance with the Guidelines for Animal Experimentation and approved by the Ethical Committee of the Faculty of Medicine at South Valley University in Qena, Egypt (Approval Code: SVU/FODM/OBID 4-23-12-764). All procedures adhered to the 2011 World Health Organization recommendations, ensuring compliance with ethical and scientific standards.

Funding Statement

None.

Conflicts of Interest

The authors declare no conflicts of interest.

REFERENCES

1. Karalliedde J, Gnudi L. Diabetes mellitus, a complex and heterogeneous disease, and the role of insulin resistance as a determinant of diabetic kidney disease. Vol. 31, Nephrology Dialysis Transplantation. Oxford University Press; 2016. p. 206–13.
2. Sun H, Saeedi P, Karuranga S, Pinkepank M, Ogurtsova K, Duncan BB, et al. IDF Diabetes Atlas: Global, regional and country-level diabetes prevalence estimates for 2021 and projections for 2045. Diabetes Res Clin Pract. 2022 Jan 1;183.
3. Verhulst MJL, Loos BG, Gerdes VEA, Teeuw WJ. Evaluating all potential oral complications of diabetes mellitus. Vol. 10, Frontiers in Endocrinology. Frontiers Media S.A.; 2019.
4. El-Sakhawy MA, Al-Sabaa A, Abusaida H, Issa Y, Moheb M. Immunohistochemical expression of Proliferating Cell Nuclear Antigen (PCNA) in the parotid salivary glands of male albino rats after long administration of nutmeg. Res J Pharm Biol Chem Sci. 2016;7(5):187–99.
5. Yasser S, Shon AA. Histomorphometric and immunohistochemical study comparing the effect of diabetes mellitus on the acini of the sublingual and submandibular salivary glands of albino rats. Open Access Maced J Med Sci. 2020;8(A):49–54.
6. Marton LT, Pescinini-e-Salzedas LM, Camargo MEC, Barbalho SM, Haber JF do. S, Sinatora RV, et al.

The Effects of Curcumin on Diabetes Mellitus: A Systematic Review. Vol. 12, Frontiers in Endocrinology. Frontiers Media S.A.; 2021.

7. Araghi A, Nazaktabar A, Sayrafi R, Salehi A, Golshahi H, Jahanbakhsh M, et al. The effects of in ovo nanocurcumin administration on oxidative stress and histology of embryonic chicken heart. Poult Sci J. 2017 Jun 1;5(2):23–9.
8. Ranjbar A, Gholami L, Ghasemi H, Kheiripour N. EEffects of nano-curcumin and curcumin on the oxidant and antioxidant system of the liver mitochondria in aluminum phosphide-induced experimental toxicity. Nanomedicine J. 2020 Jan 1;7(1):58–64.
9. El Shahawy M, El Deeb M. Assessment of the possible ameliorative effect of curcumin nanoformulation on the submandibular salivary gland of alloxan-induced diabetes in a rat model (Light microscopic and ultrastructural study). Saudi Dent J. 2022 Jul 1;34(5):375–84.
10. Ighodaro OM, Adeosun AM, Akinloye OA. Alloxan-induced diabetes, a common model for evaluating the glycemic-control potential of therapeutic compounds and plants extracts in experimental studies. Med. 2017;53(6):365–74.
11. Ashrafi P, Jahromy MH. Potential efficacy of nanocurcumin on levodopa-induced dyskinesia in a rat parkinsonian model. Phytomedicine Plus. 2022;2(4):100334.
12. Syrbu SI, Cohen MB. An enhanced antigen-retrieval protocol for immunohistochemical staining of formalin-fixed, paraffin-embedded tissues. Methods Mol Biol. 2011;717:101–10.
13. Arafa M, Raghib A, Wahba O. Immunohistochemical expression of minichromosome maintenance-3 protein in pleomorphic adenoma and mucoepidermoid carcinoma. Tanta Dent J. 2019;16(2):99.
14. Kanwal Q, Ahmed M, Hamza M, Ahmad M, Atiq-ur-Rehman, Yousaf N, et al. Curcumin nanoparticles: physicochemical fabrication, characterization, antioxidant, enzyme inhibition, molecular docking and simulation studies. RSC Adv. 2023;13(32):22268–80.
15. Scherrer P. Bestimmung der Größe und der inneren Struktur von Kolloidteilchen mittels Röntgenstrahlen. Nachrichten von der Gesellschaft der Wissenschaften zu Göttingen, Math Klasse. 1918;98.
16. Priyadarsini KI. The chemistry of curcumin: From extraction to therapeutic agent. Molecules. 2014;19(12):20091–112.
17. Lilliu MA, Loy F, Cossu M, Solinas P, Isola R, Isola M. Morphometric Study of Diabetes Related Alterations in Human Parotid Gland and Comparison with Submandibular Gland. Anat Rec. 2015;298(11):1911–8.
18. Chen S, Wang Y, Zhang C, Yang Z. Decreased basal and stimulated salivary parameters by histopathological lesions and secretory dysfunction of parotid and submandibular glands in rats with type 2 diabetes. Exp Ther Med. 2020;19:2707–19.
19. Alqahtani MS, Hassan SS. Immunohistochemical Evaluation of the Pathological Effects of Diabetes Mellitus on the Major Salivary Glands of Albino Rats. Eur J Dent. 2023;17(2):485–91.
20. Rabea AA. Comparative study on the possible effect of cod liver oil versus insulin on parotid salivary glands of streptozotocin-induced diabetic albino rats. Egypt Dent J. 2017;63:439–67.
21. Mubarak RT. Effect of Energy Drink on Rats' Submandibular Salivary Glands. Int Dent J. 2024;74:S208.
22. Lilliu MA, Solinas P, Cossu M, Puxeddu R, Loy F, Isola R, et al. Diabetes causes morphological changes in human submandibular gland: A morphometric study. J Oral Pathol Med. 2015;44(4):291–5.
23. Anderson LC, Garrett JR. Lipid accumulation in the major salivary glands of streptozotocin-diabetic rats. Arch Oral Biol. 1986;31(7):469–75.
24. Matczuk J, Zalewska A, Lukaszuk B, Knaś M, Maciejczyk M, Garbowska M, et al. Insulin Resistance and Obesity Affect Lipid Profile in the Salivary Glands. J Diabetes Res. 2016;2016:8163474.
25. Morsy MM, Ali O, Mostafa A, Ibrahim F, Hassan HA, Alabassery N. Histological and immunohistochemical study on the possible ameliorating effects of antox on the parotid gland of rats with streptozotocin-induced diabetes mellitus type 1. Egypt Soc Clin Toxicol J. 2023;11(1):12–29.
26. Sheibani M, Dehpour AR, Nezamoleslami S, Mousavi SE, Jafari MR, Sorkhabadi SMR. The protective effects of curcumin and curmumin nanomicelle against cirrhotic cardiomyopathy in bile duct-ligated rats. Nanomedicine J. 2020;7(2):158–69.
27. Kheiripour N, Plarak A, Heshmati A, Asl SS, Mehri F, Ebadollahi-Natanzi A, et al. Evaluation of the hepatoprotective effects of curcumin and nanocurcumin against paraquat-induced liver injury in rats: Modulation

of oxidative stress and Nrf2 pathway. J Biochem Mol Toxicol. 2021;35(5):1–9.

28. Hamed AM, Elbahy DA, Ahmed AR, Thabet SA, Refaei RA, Ragab I, et al. Comparison of the efficacy of curcumin and its nano formulation on dexamethasone-induced hepatic steatosis, dyslipidemia, and hyperglycemia in Wistar rats. Heliyon. 2024;10(24):e41043.

29. Bertoncini-Silva C, Vlad A, Ricciarelli R, Giacomo Fassini P, Suen VMM, Zingg JM. Enhancing the Bioavailability and Bioactivity of Curcumin for Disease Prevention and Treatment. Antioxidants. 2024;13(3).

30. Sumitomo S, Hashimura K, Mori M. Growth pattern of experimental squamous cell carcinoma in rat submandibular glands--an immunohistochemical evaluation. Eur J Cancer B Oral Oncol. 1996 Mar;32B(2):97–105.

31. Grundmann O, Mitchell GC, Limesand KH. Sensitivity of salivary glands to radiation: from animal models to therapies. J Dent Res. 2009 Oct;88(10):894–903.

32. Strzalka W, Ziemienowicz A. Proliferating cell nuclear antigen (PCNA): A key factor in DNA replication and cell cycle regulation. Ann Bot. 2011;107(7):1127–40.